GRAS SAF Report 11
Ref: SAF/GRAS/METO/REP/GSR/011
Web: www.grassaf.org
Date: 19 April 2010

The EUMETSAT Network of Satellite Application Facilities

GRAS SAF
GRAS Meteorology

GRAS SAF Report 11

ROPP 1dVar validation

Huw Lewis

Met Office, UK

Document Author Table

	Name	Function	Date	Comments
Prepared by:	H. Lewis	GRAS SAF Project Team	19 April 2010	
Reviewed by:	M. Rennie	GRAS SAF Project Team	19 Feb 2010	
Approved by:	K.B. Lauritsen	GRAS SAF Project Manager	19 April 2010	

Document Change Record

Issue/Revision	Date	By	Description
Version 1.0	19 February 2010	HL	First version
Version 1.0.1	24 March 2010	HL	Minor review edits
Version 1.0.2	19 April 2010	HL	Minor review edits

GRAS SAF Project

The GRAS SAF is a EUMETSAT-funded project responsible for operational processing of GRAS radio occultation data from the Metop satellites. The GRAS SAF delivers bending angle, refractivity, temperature, pressure, and humidity profiles in near-real time and offline for NWP and climate users. The offline profiles are further processed into climate products consisting of gridded monthly zonal means of bending angle, refractivity, temperature, humidity, and geopotential heights together with error descriptions.

The GRAS SAF also maintains the Radio Occultation Processing Package (ROPP) which contains software modules that will aid users wishing to process, quality-control and assimilate radio occultation data from any radio occultation mission into NWP and other models.

The GRAS SAF Leading Entity is the Danish Meteorological Institute (DMI), with Cooperating Entities: i) European Centre for Medium-Range Weather Forecasts (ECMWF) in Reading, United Kingdom, ii) Institut D'Estudis Espacials de Catalunya (IEEC) in Barcelona, Spain, and iii) Met Office in Exeter, United Kingdom. To get access to our products or to read more about the project please go to http://www.grassaf.org.

Abstract

The ROPP 1dVar processing is used to perform retrievals using one day of GRAS refractivity observations and ECMWF background data. Results illustrate the ROPP functionality and the output diagnostics generated. Tests using different configuration parameter settings and the error descriptions for optimal solutions are discussed. Results processed using COSMIC occulations and Met Office forecast model background data are also presented.

1 Background

The Radio Occultation Processing Package (ROPP) software includes functionality for users to perform 1dVar retrievals using refractivity or bending angle observations from GPS radio occultation (GRAS SAF, 2009a). ROPP is used to compute the GRAS SAF NRT products of temperature profile (GRM-02), specific humidity profile (GRM-03), pressure profile (GRM-04) and surface pressure (GRM-05) derived from refractivity observations. Further details of the GRAS SAF 1dVar processing is available in GRAS SAF (2009c).

This report presents refractivity and bending angle 1dVar results processed using the ROPP (v4.0) tools `ropp_1dvar_refrac` and `ropp_1dvar_bangle`. Sensitivity of results to the choice of setup parameters and assumed errors are presented. This serves to illustrate the use of ROPP for 1dVar applications and aid users to interpret the output. For further background and a full description of the ROPP 1dVar processing and user options see GRAS SAF (2009a). This report is also based on work described by GRAS SAF (2009d).

1.1 1dVar processing

The 1dVar processing aims to finds a maximum likelihood estimate of a vertical atmospheric profile $\mathbf{x}$, given a set of m observations $\mathbf{y}_o$ and some a priori knowledge of the background atmospheric state $\mathbf{x}_b$ (e.g. Lorenc, 1986). This is usually formulated as a minimisation problem of the cost function

$$J(\mathbf{x}) = \frac{1}{2}(\mathbf{x}-\mathbf{x}_b)^T\mathbf{B}^{-1}(\mathbf{x}-\mathbf{x}_b) + \frac{1}{2}(\mathbf{y}_o-\mathbf{H}[\mathbf{x}])^T\mathbf{O}^{-1}(\mathbf{y}_o-\mathbf{H}[\mathbf{x}]) \tag{1.1}$$

$\mathbf{H}[\mathbf{x}]$ denotes a (possibly nonlinear) forward operator calculating what a measurement $\mathbf{y}$ would be for any given atmospheric state $\mathbf{x}$. The matrices $\mathbf{B}$ and $\mathbf{O}$ are error covariance matrices, describing the assumed uncertainties in the background data and the measurements and forward operator respectively. By minimising J with respect to the state vector $\mathbf{x}$, we obtain a solution that minimises the total deviation against background and observational data. If all errors are normally distributed and both background and measurements are unbiased, this solution is also the maximum likelihood solution.

1.2 Input data

1.2.1 Observations

Radio occultation observation data from GRAS from 1 April 2009 were used. The 1dVar processing with a refractivity profile as the observable used the GRAS SAF GRM-01 NRT refractivity product as a function of geopotential height while the 1dVar processing with a

bending angle profile as the observable used the corresponding bending angles as a function of impact parameter as processed by EUMETSAT. In both cases, profiles were first thinned onto a set of 247 pre-defined levels using the ROPP thinner routines.

Some results are also presented using refractivity and bending angle observations on 1 April 2009 from the COSMIC mission as processed by CDAAC. These data are output on 300 levels by CDAAC.

1.2.2 Observation error

Observation standard deviations were generated using `ropp_1dvar_add_refrac_error` and `ropp_1dvar_add_bangle_error` tools provided with the ROPP distribution. Two different observation error models were tested.

1. GRAS SAF GRM-07 prototype - observation standard deviations derived using GRAS SAF NRT data processing method ('TP'). Termed 'GRAS SAF' in this report.
2. Operational model - observation standard deviations based on error structures used in operational NWP assimilation at ECMWF and Met Office ('MO', 'EC'). Termed 'NWP' in this report.

Figure 1.1 shows a plot of the assumed observation errors.

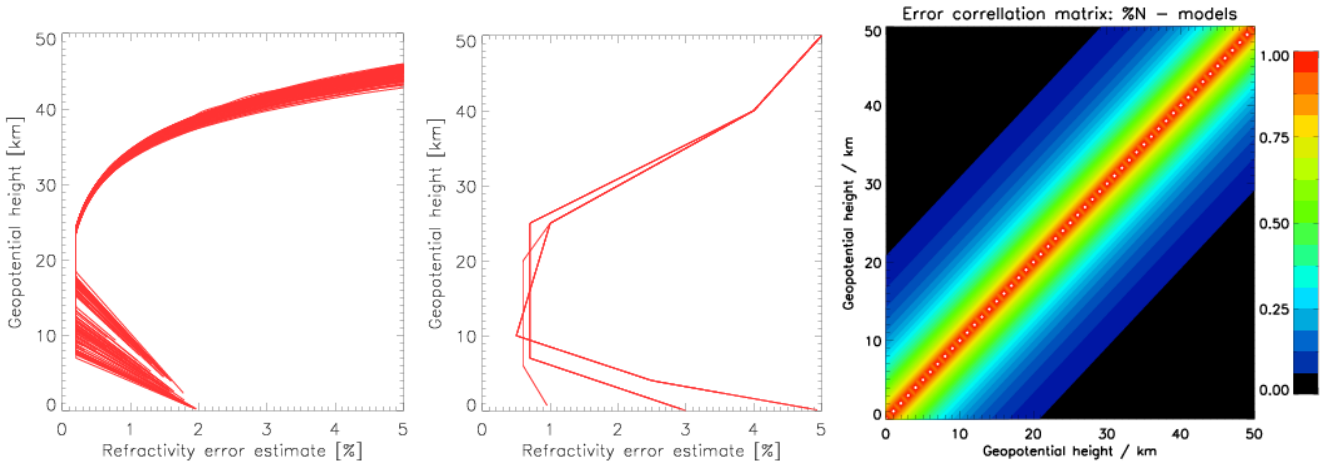

Figure 1.1: Fractional refractivity error estimates using (a) GRAS SAF tropopause height error model and (b) Met Office operational latitudinally-varying error model. (c) Assumed refractivity vertical correlations.

The same observation correlation matrix was used for both error models. For 1dVar using the refractivity observable an observation correlation matrix was defined as

$$corr_{nm} = e^{-(z_n - z_m)/H}$$

where z_n and z_m are geopotential heights at points n and m along the profile and H is a characteristic scale height of 3 km.

For 1dVar processing using a bending angle observable, the observations at different levels are considered to be uncorrelated such that the observation covariance matrix is diagonal.

1.2.3 Background profiles

Tests were conducted using background data from the ECMWF global NWP forecast model. Data are provided on 91 pressure-based model levels and the state vector consists of temperature and specific humidity on each model level and surface pressure. Model fields from the most recent ECMWF forecast at the closest 3-hourly timestep are linearly interpolated to the same geographic location as an occultation. No time interpolation is performed. These data are provided to users by the GRAS SAF ('`atm`' files) and are available online (http://www.grassaf.org).

Some results are also presented using background data from the Met Office global forecast model. In April 2009, data were provided on 50 geopotential height-based model levels up to a model top of about 65 km. The state vector consists of 50 specific humidity values (defined on the 'θ' model levels) and 51 pressure values (on the 'ρ' model levels).

1.2.4 Background errors

Two different background error models for ECMWF data were tested.

1. GRAS SAF 1dVar prototype - mean of profile-by-profile background errors used in GRAS SAF NRT 1dVar processing based on 'error of the first guess' variable. The error estimate on surface pressure is set constant to 1 hPa. Termed 'GRAS SAF' in this report. (See Figure 1.2).

2. Operational model - assumed global mean background errors provided by Mike Fisher (ECMWF). The surface pressure error estimate is 1.2 hPa. Termed 'NWP' in this report. (See Figure 1.2).

The GRAS SAF method produces temperature and specific humidity background errors which are about twice the magnitude of the operational model, leading to larger weighting of observations in the 1dVar retrieval. Note that only an approximate mean error distribution was used in this analysis. The GRAS SAF NRT 1dVar processing uses an error description which varies profile-by-profile. Results reported here are therefore not entirely analogous to the GRAS SAF NRT products.

In both cases, the same correlations between model levels were used and it is assumed that there are no cross-correlations between temperature, humidity and surface pressure (Figure 1.3).

For tests using Met Office background data, the assumed background errors and correlations used in the Met Office operational processing were used (Figure 1.4). Different errors are defined for the northern hemisphere, tropics and southern hemisphere regions.

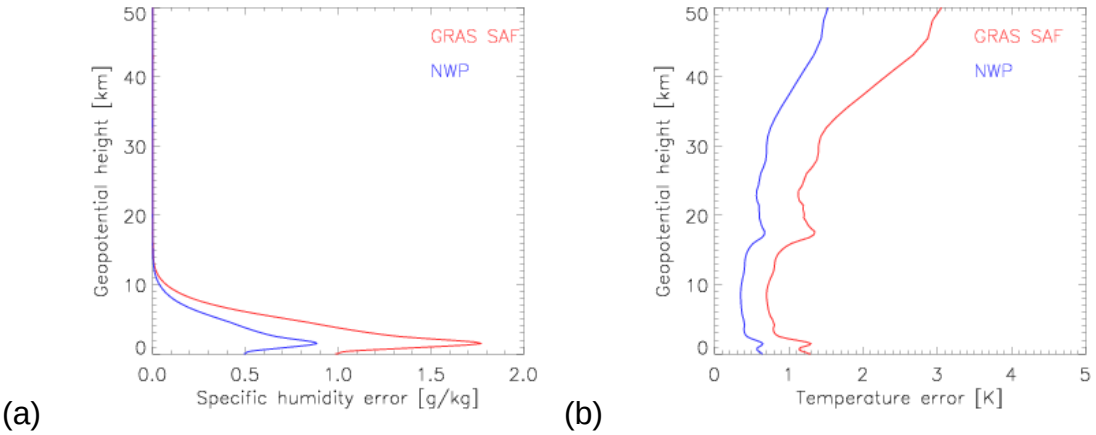

Figure 1.2: Assumed ECMWF model background errors for (a) specific humidity and (b) temperature. The 'NWP' assumed errors are plotted in blue (surface pressure error 1.2 hPa), the 'GRAS SAF' assumed errors are plotted in red (surface pressure error 1.0 hPa).

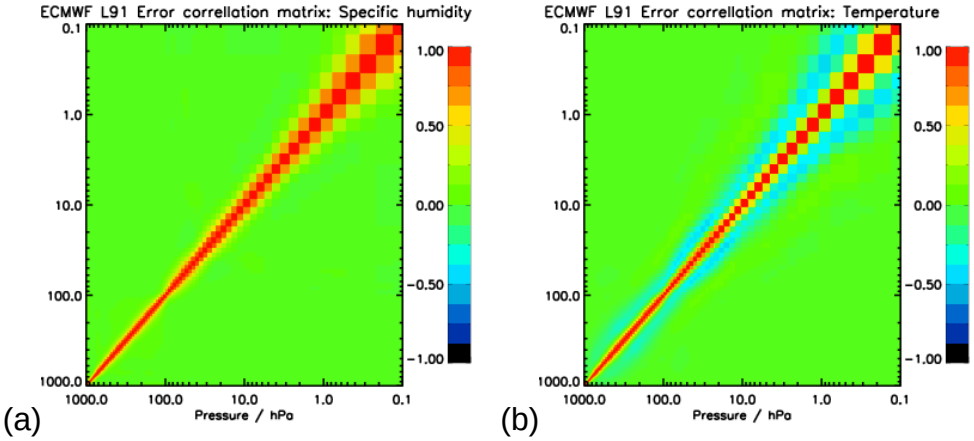

Figure 1.3: Assumed ECMWF model background vertical correlations for (a) specific humidity and (b) temperature.

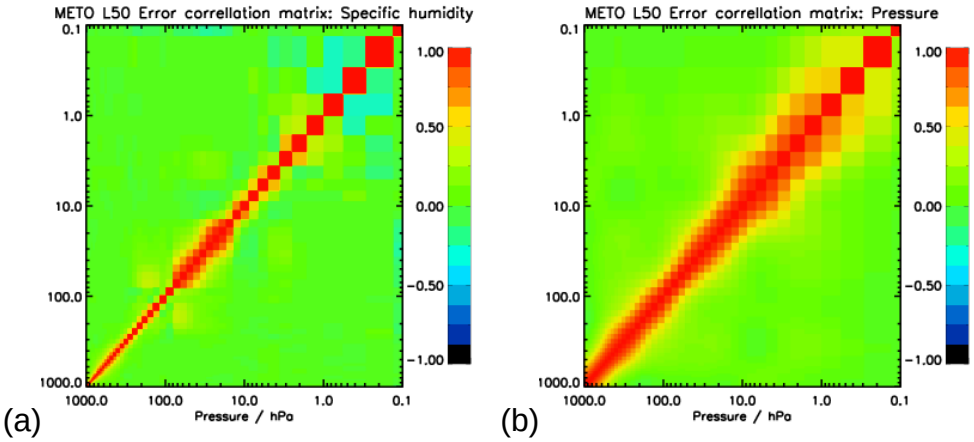

Figure 1.4: Assumed Met Office model background vertical correlations (in the tropics) for (a) specific humidity and (b) temperature.

1.3 Configuration options

Except where stated, the following user-configurable parameters were used in the ROPP processing (see GRAS SAF (2009a) for further details).

A series of tests were conducted to assess the choice of parameters used.

1. Minimiser algorithm: by default quasi-Newton minimisation (`minROPP`) was used. Tests were repeated using the Levenberg-Marquardt (`LevMarq`) algorithm. GRAS SAF (2008) provides some example comparisons of 1dVar solutions generated using the two approaches.
2. Data cutoff limits: by default only GRAS observations between 8 (`min_1dvar_height`) and 35 km (`max_1dvar_height`) were used in the 1dVar analysis. Tests were also conducted using all data.
3. Pressure and humidity state variable: by default pressure and specific humidity are used in the state vector. Tests were also conducted using $ln(p)$ and $ln(q)$ as state vector variables (`use_logp = .true.`, `use_logq = .true.`).

VarConfig		
Structure element	Default	Description
...%obs_covar_method	VSFC	Observation error covariance method
...%bg_covar_method	VSFC	Background error covariance method
...%min_1dvar_height	8 km	Min. obs height to include in 1d–Var
...%max_1dvar_height	35 km	Max. obs height to include in 1d–Var
...%bgqc_apply	.true.	Apply background quality control?
...%bgqc_reject_factor	10	Data rejected if O-B $>$ factor * observation standard deviation
...%bgqc_reject_max_percent	50	Maximum % of data rejected
...%pge_apply	.false.	Apply PGE for quality control?
...%minROPP%method	MINROPP	minimisation method
...%use_precond	.true.	Use preconditioning?
...%conv_check_apply	.true.	Apply additional convergence checks?
...%conv_check_n_previous	2	Consecutive iterations for convergence
...%conv_check_max_delta_state	0.1	Maximum change in state vector
...%conv_check_max_delta_J	0.1	Maximum change in cost function
...%extended_1dvar_diag	.true.	Output additional diagnostics?
...%use_logp	.false.	Use Log(pressure) in state vector for 1D–Var?
...%use_logq	.false.	Use Log(humidity) in state vector for 1D–Var?

Table 1.1: Configuration options used in 1dVar processing. All other configuration parameters are as defaults listed in (GRAS SAF, 2009a).

2 Results: GRAS refractivity, ECMWF background

This section describes quality control and validation of the 1dVar processing applied to 621 GRAS occultations from 1st April 2009 and co-located background data from ECMWF forecasts (analysis cycle 35r2). Figures summarise results from a number of different tests conducted (see Section 1).

Of 621 profiles processed, 597 passed initial quality control checks (e.g. $O-B$ checks, data range checks). Figure 2.1 shows statistics of the relative difference between GRAS refractivity observations and the forward-modelled ECMWF background (black = $(\mathbf{y}_o - \mathbf{H}[\mathbf{x}_b])/\mathbf{H}[\mathbf{x}_b]$). These are consistent with the data quality monitoring plots available at http://www.grassaf.org. Biases are smallest between 10 and 35 km, increasing at high altitudes where the refractivity data are merged with climatology. Also shown in Figure 2.1 are statistics of the relative difference between the GRAS observations and the forward-modelled 1dVar solution (red = $(\mathbf{y}_o - \mathbf{H}[\mathbf{x}])/\mathbf{H}[\mathbf{x}]$). This illustrates how the 1dVar processing draws the background state towards the observations over the 8 to 35 km height range used in the analysis.

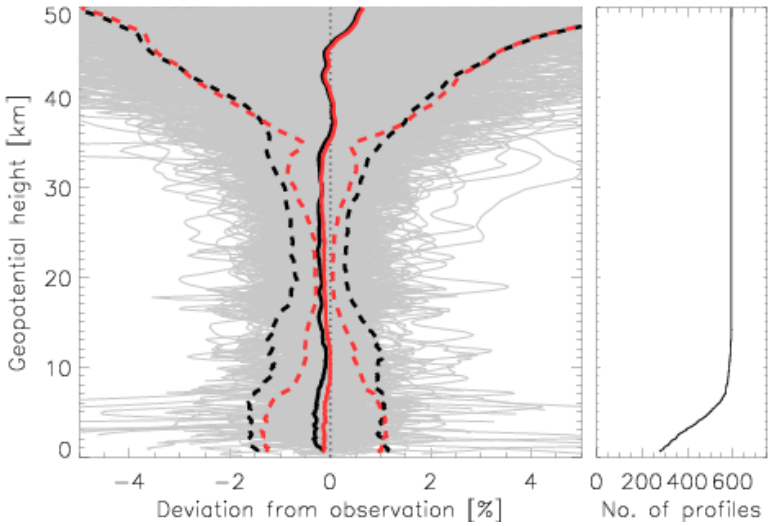

Figure 2.1: Profiles of relative differences between observation and background refractivity ('[O-B]/B'). The mean bias [O-B]/B (solid black line) and bias $\pm$ standard deviation (dotted black line) are plotted. Also shown is the mean bias [O-A]/A (solid red line) and bias $\pm$ standard deviation (dotted red line), where 'A' is the 1dVar solution.

2.1 Quality at convergence measures

Convergence is assumed when either the state vector changes by less than the parameter value `conv_check_max_delta_state` times the background error or if the cost function changes by less than `conv_check_max_delta_J` between successive iterations.

Number of iterations

Figure 2.2 illustrates that the `minROPP` minimisation algorithm typically converges to a solution after between 8 and 15 iterations using the 'GRAS SAF' set of assumed background and observation errors. The distribution is much more strongly peaked at 6 iterations when using the 'NWP' assumed errors. The Levenberg-Marquardt minimisation algorithm typically converges to a solution in 3 iterations (as illustrated by GRAS SAF (2008) for example).

The GRAS SAF NRT 1dVar processing chain (GRAS SAF, 2009c) uses a number of 1dVar diagnostic criteria to assess the quality of the output. Profiles are flagged as bad if:

1. The normalised cost function $2J/m$ value is greater than 5.
2. The minimiser uses more than 25 iterations to converge.
3. The specific humidity at any point in the profile is above saturation.
4. The input refractivity profile was marked as bad.

These criteria are checked in the ROPP 1dVar processing and bad profiles are indicated by setting the `PCD_met` bit of the product confidence data (PCD) output variable as non-nominal and the `overall_qual` variable to zero (GRAS SAF, 2009b).

Of 597 profiles for which the minimisation was attempted with the default configuration settings and GRAS SAF assumed errors, 1 (0.17%) failed due to $2J/m$ exceeding 5, and 2 (0.33%) failed due to the minimisation not reaching convergence (within 50 iterations). This is consistent with the results of GRAS SAF (2009d) from an analysis using a month of data. A significantly higher proportion of profiles (3.01%) failed the $2J/m$ test when using the `LevMarq` minimiser with the GRAS SAF errors. However, when using `LevMarq` with NWP assumed errors, the proportion of profiles failing the $2J/m$ test was only 0.5%.

Cost function at convergence, $2J/m$

Figure 2.2 shows histograms of $2J/m$ values (middle column) and the latitude dependence of $2J/m$ (right column). Here, J is the cost function at convergence and m is the number of observations used in the analysis. If the distribution of observation and background data is perfectly Gaussian, unbiased and well described by the covariance matrices then $2J/m$ should have a value of 1.0. For all cases tested, the majority of occultations have $2J/m$ less than 1.0. Results using the GRAS SAF assumed errors have significantly larger spread of $2J/m$ values than those obtained using NWP assumed errors. There are no significant differences between the distribution of $2J/m$ values due to the choice of minimiser algorithm or humidity state vector variable. Results of tests using observation data from all available altitudes in the 1dVar analysis (not shown) are also generally similar.

(a) 'GRAS SAF' errors, (p,q) state variables, `minROPP` minimisation

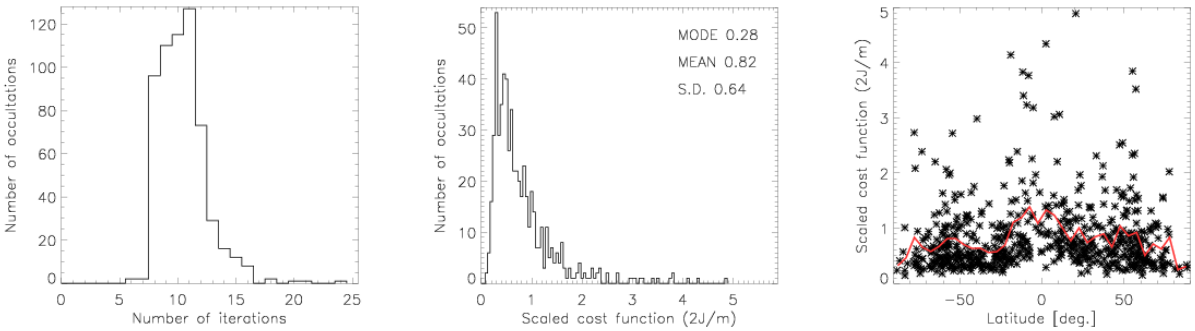

(b) 'GRAS SAF' errors, $\ln(p,q)$ state variables, `minROPP` minimisation

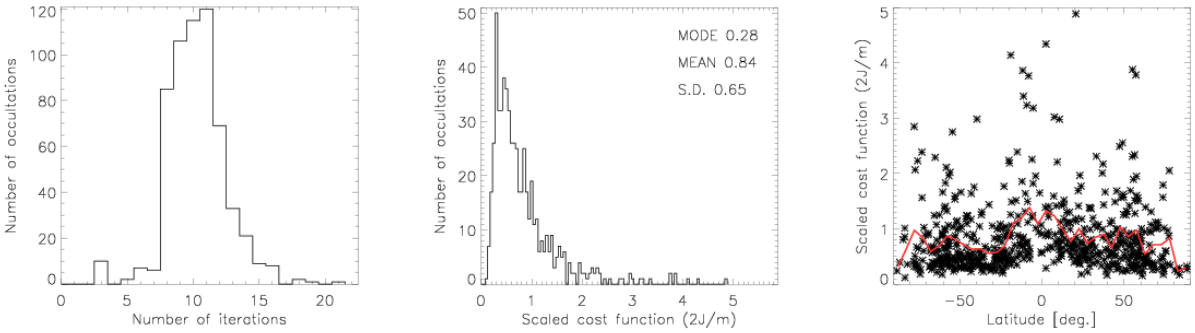

(c) 'GRAS SAF' errors, (p,q) state variables, `LevMarq` minimisation

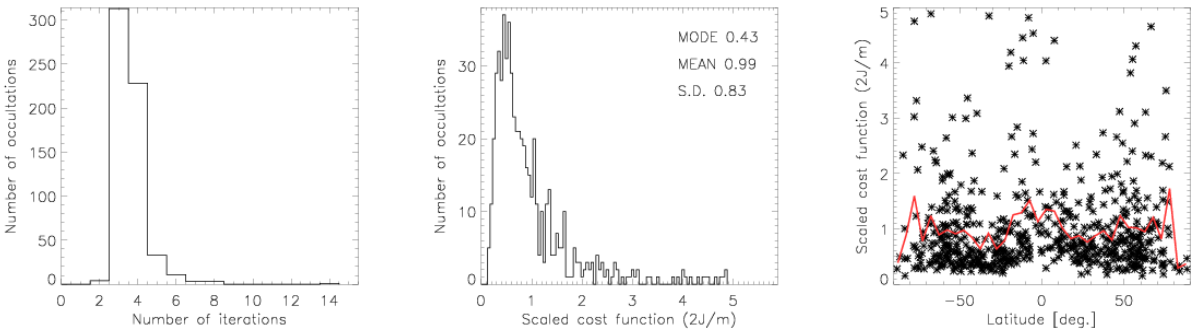

(d) 'NWP' errors, (p,q) state variables, `minROPP` minimisation

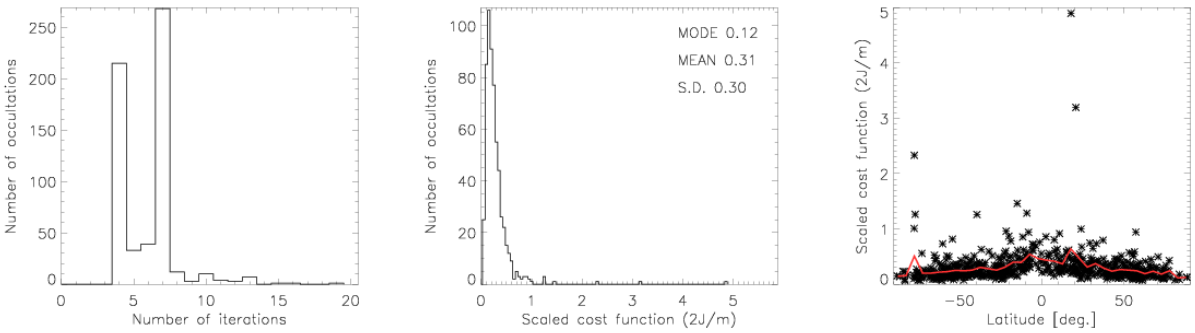

Figure 2.2: left column: Number of iterations required for convergence. (Note different scales on each plot). middle column: histogram of $2J/m$ values at convergence. right column: distribution of $2J/m$ with latitude. The zonal mean is plotted as a solid (red) line.

Altitude dependence of J

The cost function J (Equation 1.1) represents a summation of deviations of the solution state from the background and the forward-modelled solution state from the observations (GRAS SAF, 2009a). The contribution to the cost function from each element of the observation and background vectors may be described by calculating,

$$J_{obs}(i) = \frac{1}{2}(y_o(i) - \mathbf{H}[\mathbf{x}]_i).\left[\mathbf{O}^{-1}(\mathbf{y}_o - \mathbf{H}[\mathbf{x}])\right] \quad (2.1)$$

$$J_{bgr}(j) = \frac{1}{2}(x(j) - x_b(j)).\left[\mathbf{B}^{-1}(\mathbf{x} - \mathbf{x}_b)\right] \quad (2.2)$$

The contribution for each element in the observation or state vector can then be related to the altitude of that element. Note that values may be positive or negative.

Figure 2.3 shows the mean profile of cost function contributions, normalised by the total J value (Equation 1.1) for each occultation. The state vector part is further split into the contributions for each temperature and specific humidity element. Use of data between 8 km and 35 km restricts contributions from J_{obs} to between these altitudes. The distribution of J_{obs} and J_{bgr} results from a balance between the vertical distributions of the assumed errors and the fit of observations to the background. Rapidly increasing observation errors above 25 km and below 10 km results in a drop-off of contributions to J_{bgr} and J_{obs} since increments of the state vector from the initial background are reduced. In the upper troposphere and lower stratosphere the RO observations are well matched to the initial background state, so contributions to J_{obs} and J_{bgr} are reduced here and there is a minimum around 17 km. The largest contributions to J_{obs} originate from the troposphere between 8 and 12 km where observation errors are relatively small but biases between observations and the initial background state may be relatively large for some occultations. Largest contributions to J_{bgr} (for temperature) originate from the stratosphere between 20 and 30 km where differences between the observations and background are increased (and thus increments from the background state are increased) but the assumed errors are relatively small. Contributions to J from the specific humidity part of the state vector are generally small. The impact of specific humidity information in the 1dVar retrieval will be increased with the availability of improved refractivity data below 8 km processed by wave optics methods.

Mean profiles of J_{obs} from all tests presented in Figure 2.3 are generally similar in magnitude and structure. Sensitivity of results to the 1dVar configuration parameters is more clearly illustrated by differences in the output J_{bgr} profiles. Specific points to note are:

1. **Minimiser algorithm**: Increased J_{bgr} standard deviations for specific humidity using the `LevMarq` minimiser compared with `minROPP`, very similar contributions from temperature and J_{obs}.

2. **State vector variables**: Increased J_{obs} standard deviations and less pronounced minimum around 17 km when using $\ln(p,q)$ state vector variables. Increased J_{bgr} (temperature) standard deviations, no influence on J_{bgr} for humidity state vector elements.

3. **Assumed errors**: Decreased background errors in the 'NWP' assumed errors setup leads to smaller increments and reduced J_{bgr} values. The bi-modal vertical distribution of temperature J_{bgr} profile resulting from 'GRAS SAF' assumed errors is smoothed out to a single peak around 20 km when using 'NWP' errors.

(a) 'GRAS SAF' errors, (p,q) state variables, `minROPP` minimisation

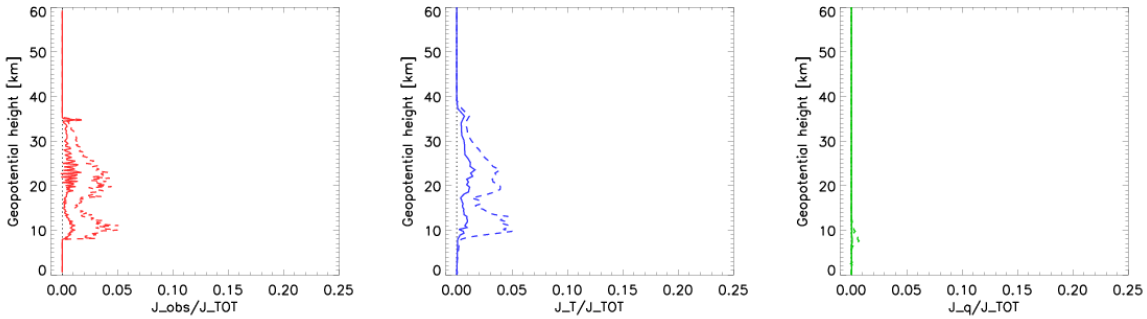

(b) 'GRAS SAF' errors, $\ln(p,q)$ state variables, `minROPP` minimisation

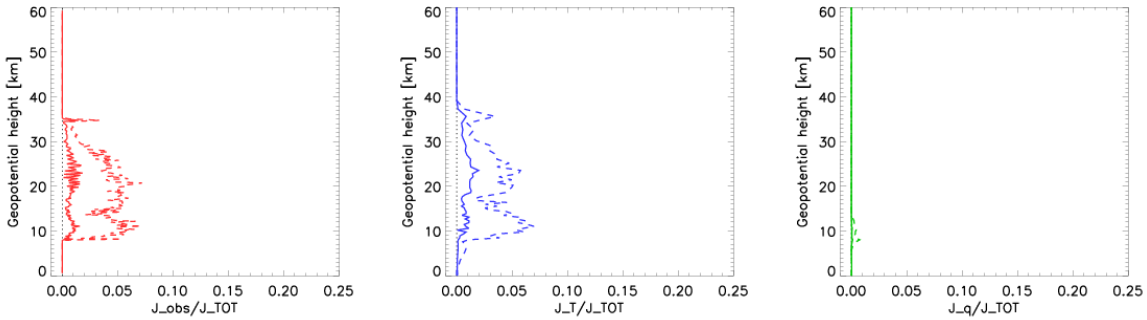

(c) 'GRAS SAF' errors, (p,q) state variables, `LevMarq` minimisation

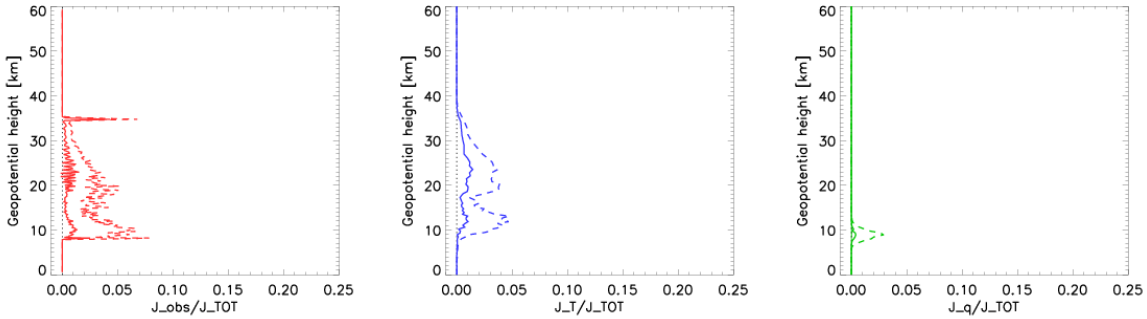

(d) 'NWP' errors, (p,q) state variables, `minROPP` minimisation

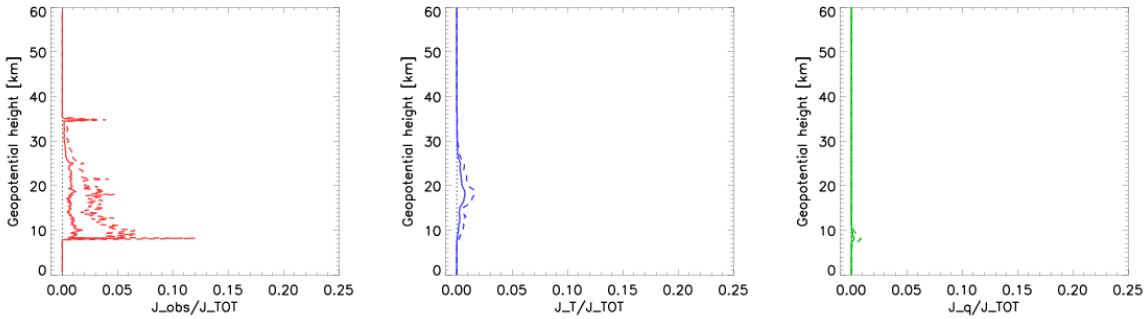

Figure 2.3: Profiles of contribution to cost function from observations (red), temperature part of background state vector (blue) and humidity part of background state vector (green). Solid line: bias, dashed line: standard deviation about the mean.

2.2 State vector solutions

Figure 2.4 shows the magnitude of increments between the temperature, specific humidity and surface pressure elements of the background ECWMF state vector and 1dVar solution.

2.2.1 Temperature

Increments are unbiased (< 0.1 K) at all altitudes and standard deviations remain within 1 K below 30 km. For the default processing setup, largest increments are seen around 35 km (at the top of the used observations window) and 17 km (where the observation errors are smallest). The temperature solutions are independent of whether (p,q) or $\ln(p,q)$ state vector variables are used. For 1dVar processing using the `LevMarq` minimiser, results are generally similar although the larger increments at 35 km are removed. Temperature increments are reduced by a factor of about 2 when using the 'NWP' assumed background and observation errors (Figure 2.4(d)), since the background is given relatively more weight in the retrieval.

2.2.2 Specific humidity

Although only observations between 8 and 35 km are used in the retrieval, large increments to the background surface humidity are apparent down to the surface. The specific humidity increments in Figure 2.4(a) show a negative bias, peaking at about 3 km with a mean value of -0.16 g/kg. Standard deviations have a maximum value of 0.29 g/kg at the same height. Use of the $\ln(p,q)$ state vector variable (Figure 2.4(b)) results in slightly reduced increments (mean -0.13 g/kg, standard deviation 0.34 g/kg). In contrast, the `LevMarq` specific humidity solutions in Figure 2.4(c) have a much smaller bias (maximum mean 0.02 g/kg, standard deviation 0.08 g/kg).

The near-surface increments are non-zero since the forward model for an ECMWF background involves integrating the hydrostatic equation to compute geopotential height (GRAS SAF, 2009a). The geopotential height calculation is related to specific humidity and temperature through the virtual temperature. Modifications to the state vector at heights where observations are included in the analysis therefore contribute to near-surface elements of the state adjoint (as used in the `minROPP` minimisation) and state tangent linear (as used in the `LevMarq` minimisation).

Result using the 'GRAS SAF' background covariance matrix and `minROPP` minimiser (Figures 2.4(a) and (b)) have been found to be strongly sensitive to the details of the preconditioning used before the minimisation. The `minROPP` minimisation is performed on a control variable, defined as

$$\mathbf{control} = \mathbf{L}^{-1}\mathbf{x} \tag{2.3}$$

where $\mathbf{L}$ is a preconditioner related to the background covariance matrix as $\mathbf{B} = \mathbf{L}\mathbf{L}^T$ (GRAS SAF, 2009a). This transformation apparently increases the impact of the background correlations on the humidity increments in particular for the given choice of $\mathbf{B}$ matrix. Figure 2.5 shows the increments obtained if only the diagonal elements of $\mathbf{B}$ were used in defining the **control** variable. In this case, the temperature and surface pressure increments are largely unaffected, but the maximum specific humidity increment is reduced to only 0.019 g/kg (standard deviation 0.06 g/kg).

(a) 'GRAS SAF' errors, (p,q) state variables, `minROPP` minimisation

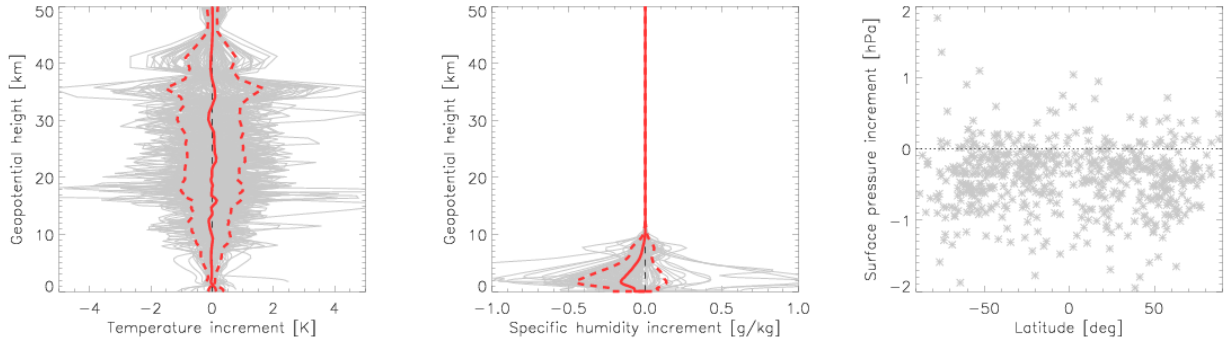

(b) 'GRAS SAF' errors, $\ln(p,q)$ state variables, `minROPP` minimisation

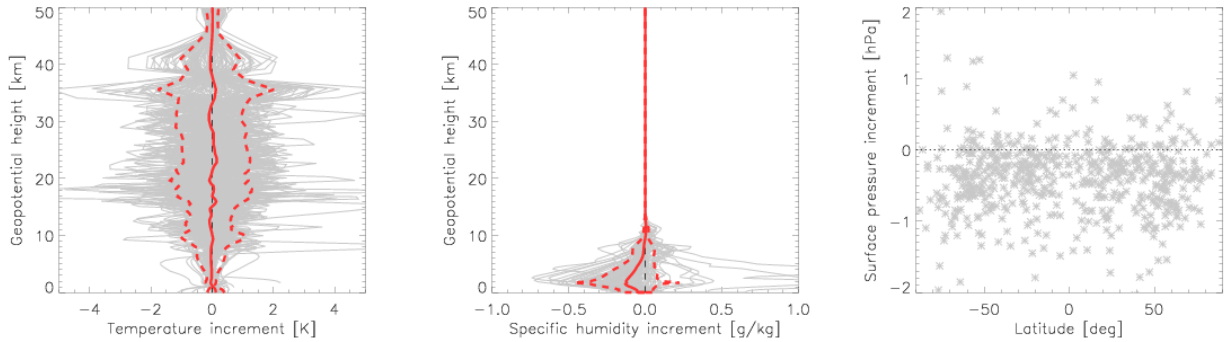

(c) 'GRAS SAF' errors, (p,q) state variables, `LevMarq` minimisation

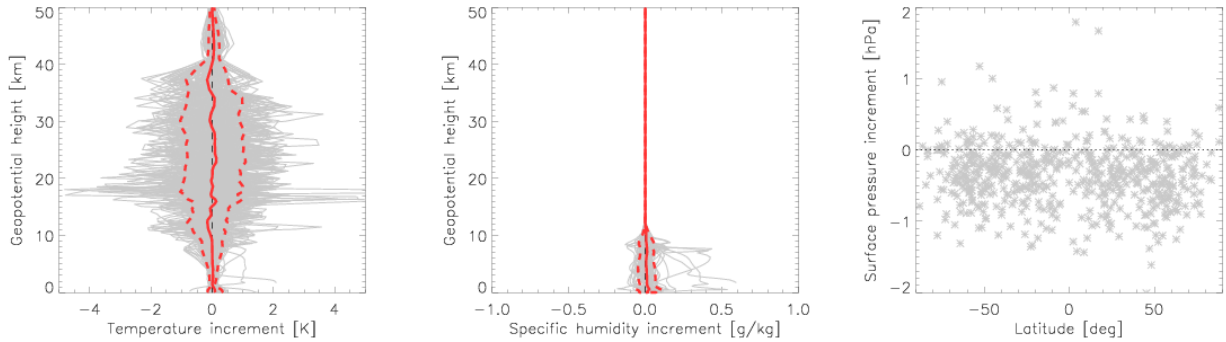

(d) 'NWP' errors, (p,q) state variables, `minROPP` minimisation

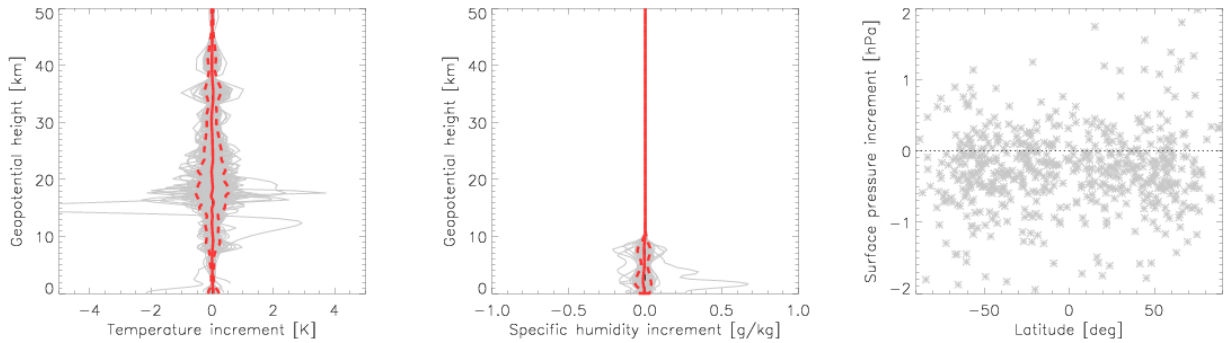

Figure 2.4: Increments of ECMWF state vector elements (1dVar solution - background) for temperature (left column), specific humidity (middle column) and surface pressure (right column). The mean and mean $\pm$ standard deviation are plotted as solid and dashed lines respectively.

(a) 'GRAS SAF' errors, (p,q) state, `minROPP` minimisation (diagonal preconditioner)

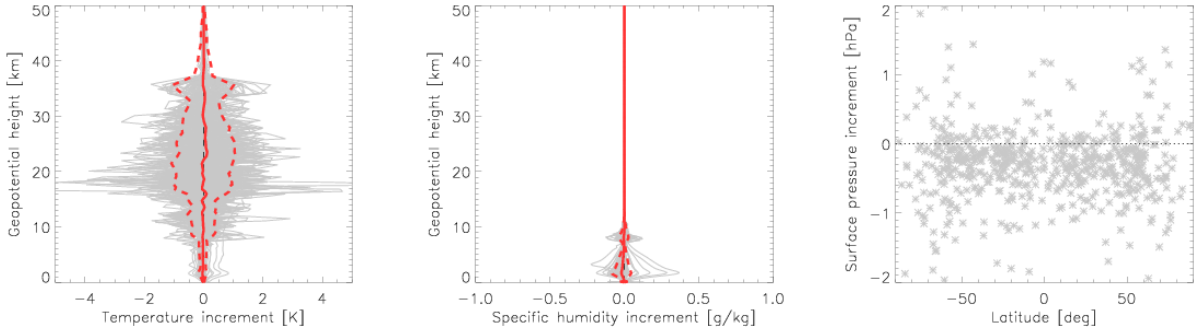

Figure 2.5: Increments of ECMWF state vector elements using only diagonal elements of $\mathbf{B}$ in the `minROPP` preconditioner. (1dVar solution - background) for temperature (left column), specific humidity (middle column) and surface pressure (right column). See Figure 2.4 for further details.

Applying the diagonal pre-conditioner to a 1dVar retrieval using the 'NWP' assumed errors led to much poorer performance however. Solutions did not differ significantly from the background, and convergence was achieved with very little reduction to the cost function. While modifying the preconditioning matrix therefore led to improved solutions for retrievals using the 'GRAS SAF' errors, it should not be considered a general solution.

The simplest option to generate solutions with small and unbiased humidity increments would be to use the `LevMarq` minimiser algorithm. The results shown in Figure 2.5 are very similar to those obtained using the `LevMarq` minimiser (Figure 2.4(c)). GRAS SAF (2008) provided some specific example 1dVar retrievals using `minROPP` and `LevMarq` (with 'NWP' assumed errors, ROPP v1.2). For some cases it was found that the `LevMarq` method produced 1dVar solutions with smaller cost function values and which deviate more from the background profiles. The `minROPP` routine was found to be typically three times faster than `LevMarq` however. For the current set of tests conducted (ROPP v4.1), the `LevMarq` processing was found to be only 25% slower than `minROPP`. The mean CPU time to process each profile was 0.96 s using `minROPP` and 1.2 s using `LevMarq`.

Users requiring the more efficient `minROPP` algorithm should consider performing a comparison of the `minROPP` and `LevMarq` solutions and, if required, adapt the definition of the preconditioner to limit any systematic features in the solution. The choice of preconditioner used for one assumed background covariance may not necessarily be appropriate for all error models. The `LevMarq` minimiser routine is recommended to most users however. The processing should currently be efficient enough for most users and no preconditioning is performed. It is planned to improve the efficiency of the `LevMarq` minimisation (for release version ROPP-5) by including a 'K-code' representation of the tangent linear routines.

2.2.3 Surface pressure

The pressure value on each ECMWF model level is defined by the surface pressure value via model level coefficients (GRAS SAF, 2009a). Profiles of the pressure increment (not shown) indicate that fractional pressure differences are limited to below 15 km, increasing to a maximum percentage difference at the surface. The right column of Figure 2.4 plots the distribution of surface pressure increments with latitude. These show a striking negative bias of about -0.4 hPa for all tests conducted using the 'GRAS SAF' assumed errors. The 1dVar solution reduced the surface pressure value for 83% of occultations. Although the bias is reduced to -0.09 hPa when using the 'NWP' errors (Figure 2.4), the surface pressure value is reduced in the solution for 70% of occultations. The surface pressure increments are not a function of latitude.

The negative surface pressure increment bias is thought to originate from the small negative refractivity bias against the ECMWF forecast background shown in Figure 2.1. At 20 km, for example, the mean $(O-B)/B$ value is -0.15%. Assuming temperature and humidity are kept constant in the analysis, it is possible to reduce the refractivity in the 1dVar solution by reducing pressure values (since refractivity is directly proportional to pressure). In the ECMWF model, all background pressure values are reduced by decreasing the surface pressure value. Decreasing pressure at each model level has the impact of increasing the heights of each level, further improving the match between the background and observed refractivity profiles in the 1dVar retrieval.

Modified bias test

To test this hypothesis, the 1dVar analysis was re-run after adding a constant 2% positive bias to the refractivity observations. Figure 2.6 shows the 1dVar solution increments for temperature, specific humidity and surface pressure. The strong positive refractivity bias is resolved by increasing the surface pressure (mean increments 3.4 hPa), which increases the pressure on each model level and decreases the height of each level. There is also some impact in increasing the tropopspheric specific humidity increments in the 1dVar solution, but not a large impact on temperature. This result supports the suggestion that the negative surface pressure increment bias shown in Figure 2.4 results from the negative $(O-B)/B$ refractivity bias.

Modified background error test

Figures 2.4 and 2.6 illustrate that biases between the initial background and observations result in relatively strong biases in surface pressure increments using the 1dVar retrieval with ECMWF model levels and state vector. A further test was therefore run applying the 1dVar retrieval with a greatly reduced estimate of the surface pressure error of 1 Pa (rather than 1 hPa). Figure 2.7 shows the 1dVar solution increments for temperature, specific humidity and surface pressure when using a surface pressure error of 1 Pa. The surface pressure element is now constrained much more closely to the background and the mean increment is 0.0025 hPa. The temperature and specific humidity increments however are remarkably similar to those shown in Figure 2.4(c) for the test using the default setup.

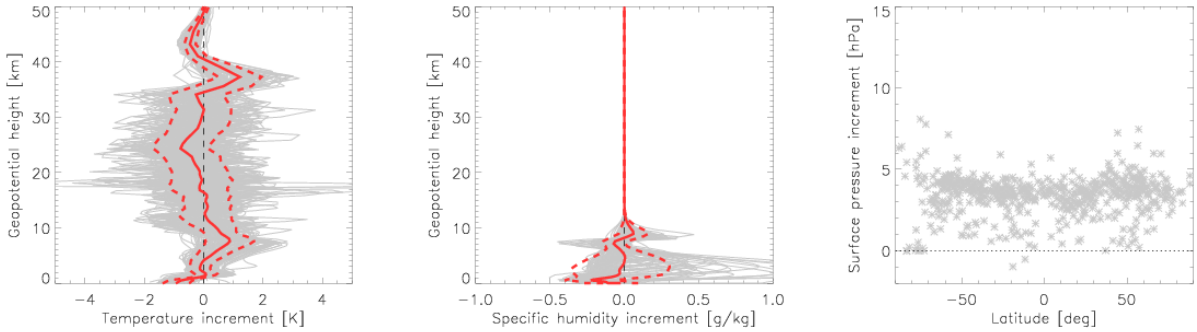

Figure 2.6: Increments of ECMWF state vector elements using 2% biased observations (1dVar solution - background) for temperature (left column), specific humidity (middle column) and surface pressure (right column). See Figure 2.4(c) for further details.

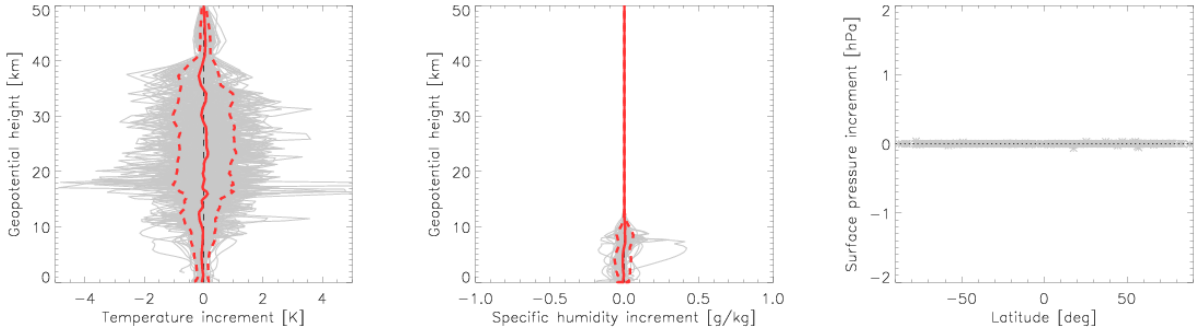

Figure 2.7: Increments of ECMWF state vector elements using 1 Pa assumed surface pressure error (1dVar solution - background) for temperature (left column), specific humidity (middle column) and surface pressure (right column). See Figure 2.4(c) for further details.

Updated ECMWF background test

An updated 1dVar test was finally run using more recent observations and ECMWF background data from 10th February 2010. From 13th October 2009, an update was made to the COSMIC RO processing (at UCAR) which led to modified ECMWF forecast biases relative to radio occultation observations. Figure 2.8 illustrates this updated bias structure for the sample day of 10th February 2010.

Figure 2.9 shows the temperature, humidity and surface pressure increments of the 1dVar solution from the ECWMF background on 10th February 2010. The temperature and specific humidity increments are generally similar to those on 1st April 2009 (Figure 2.4(c)). The mean surface pressure increment is -0.16 hPa. The surface pressure is reduced in the 1dVar solution for only 60% of occultations. The strongly negative bias is therefore reduced since the bias between ECMWF and GRAS observations has reduced. Further reductions to this bias might be anticipated when updates to the assimilation of biased aircraft temperatures are implemented at ECMWF (S. Healy, pers comm).

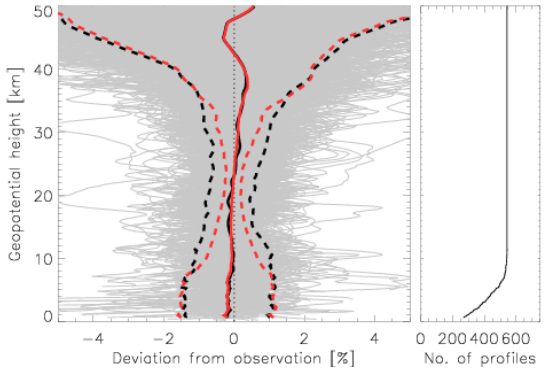

Figure 2.8: Relative differences between observation and ECMWF background refractivity ('$[O-B]/B$') for 1 day on 10th February 2010, after the ECMWF biases were adjusted by updates to the COSMIC observation processing.

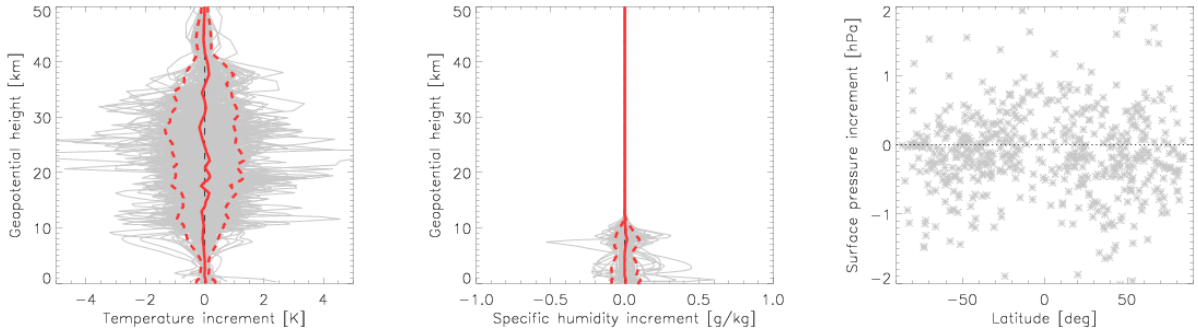

Figure 2.9: Increments of ECMWF state vector elements using data from 10th February 2010. (1dVar solution - background) for temperature (left column), specific humidity (middle column) and surface pressure (right column). See Figure 2.4 for further details.

2.3 State vector error estimates

The ROPP 1dVar processing computes estimates of the error of the solution in the form of an error covariance matrix $\mathbf{S}$. Taking the square root of the diagonal element of the covariance matrix gives and estimated standard error profile (which may be output as `temp_sigma, shum_sigma, pres_sfc_sigma` variables in an output ROPP format file).

$$\mathbf{S} = \left(\mathbf{B}^{-1} + \mathbf{H}[\mathbf{x}]\mathbf{O}^{-1}\mathbf{H}[\mathbf{x}]^{T}\right)^{-1} \tag{2.4}$$

Comparing this error with the background error estimate gives an indication of how much information was gained from the observation. Figure 2.10 shows the solution standard error profiles for tests using the default setup with 'GRAS SAF' and 'NWP' assumed background errors. These results were found to be independent of the choice of minimisation algorithm or form of humidity and pressure state vector variables. The magnitude and structure of the solution errors is very similar when using either choice of error definitions. As such, the observations are considered to provide more information to the solution when using the 'GRAS SAF' background errors than when using the smaller 'NWP' errors.

(a) 'GRAS SAF' errors, (p,q) state variables, `LevMarq` minimisation

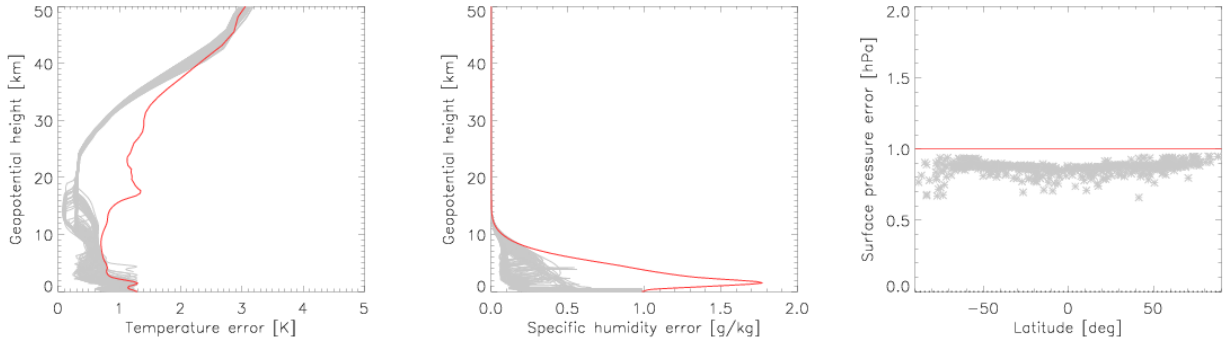

(b) 'NWP' errors, (p,q) state variables, `LevMarq` minimisation

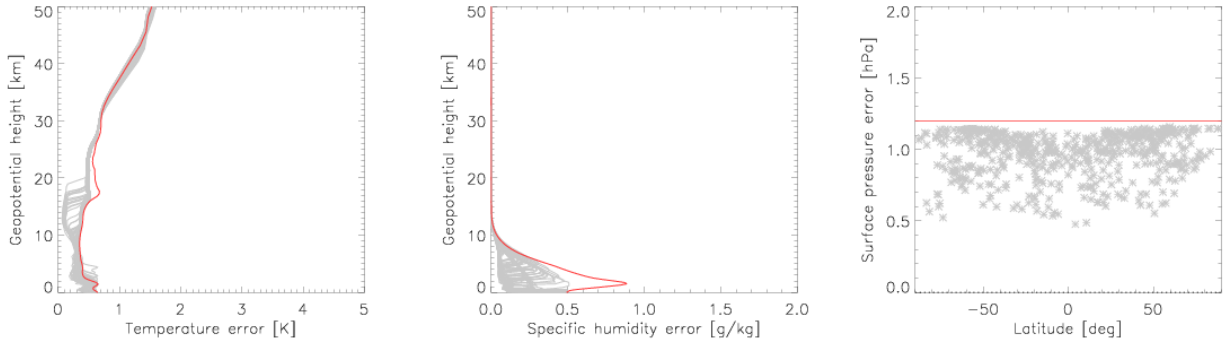

Figure 2.10: Background (red) and 1dVar solution (grey) error estimates for temperature, specific humidity and surface pressure.

2.4 Refractivity error estimates

The background and solution error covariance matrices can also be converted into estimated error covariances in refractivity-space through the tangent linear of the forward-model operator $\mathbf{H}$. Taking the square root of the diagonal element of the covariance matrix gives an estimated standard error profile (which may be output as `refrac_sigma` variable in an output ROPP format file). Note that this estimate ignores errors associated with the interpolation performed by the forward model. This results in an oscillatory structure at high-altitudes where the model levels are further apart and the interpolation is more important to the solution.

$$\mathbf{S}_o = \mathbf{H}[\mathbf{x}]\mathbf{B}\mathbf{H}[\mathbf{x}]^T \tag{2.5}$$

Figure 2.11 compares the mean assumed observation error with the background error, forward modelled into refractivity-space following Equation 2.5 (optionally output as additional diagnostic variable `B_sigma`), and the solution error. This is further demonstration of the improved solution errors in the height range 10 to 35 km, and reduced impact of observations using the 'NWP' error model.

Also plotted in Figure 2.11 are comparisons of the $(O-B)/B$ and $(O-A/A)$ standard deviations (as shown in Figure 2.1) with an estimate of the expected errors (GRAS SAF,

2009d).

$$\sigma\left[\frac{(O-B)}{B}\right] \approx \frac{\sqrt{(\sigma_o)^2 + \left(\sigma_B \frac{O}{B}\right)^2}}{B} \tag{2.6}$$

Note that O and B here denote the observation and (forward-modelled) background profiles and not the covariance matrices. The statistical and estimated curves coincide nicely in the height range 10 to 35 km in Figure 2.11(a) for the tests using the 'GRAS SAF' assumed errors. At high and low latitudes the observed standard deviations are smaller than the input error estimates. At low latitudes this is because only those profiles with high measurement quality tend to reach the surface (low humidity, no sharp refractivity gradients). At high altitudes, deliberately inflated observation errors are used so as not to introduce known observation biases into the 1dVar solution. Figure 2.11(b) shows generally smaller observed standard deviations at all altitudes when using the 'NWP' error model, since the input errors are chosen to be conservative in the amount of information provided by the observations in the solution. These results are independent of the choice of minimiser and state vector humidity and pressure variable.

(a) 'GRAS SAF' errors, (p,q) state variables, `LevMarq` minimisation

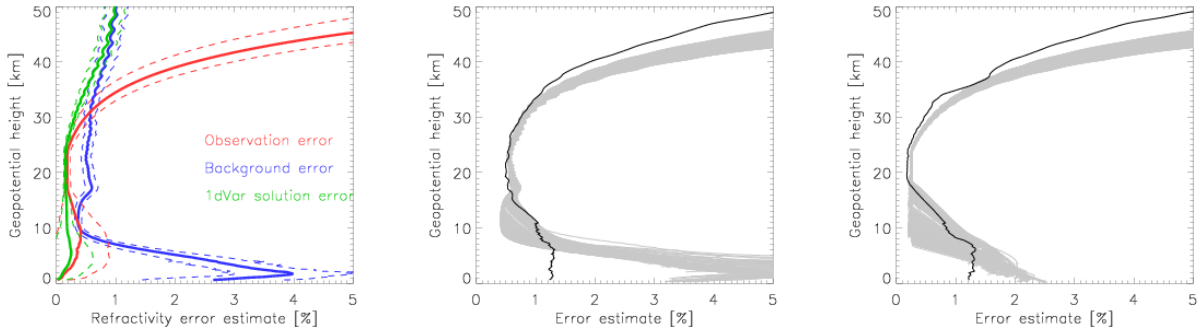

(b) 'NWP' errors, (p,q) state variables, `LevMarq` minimisation

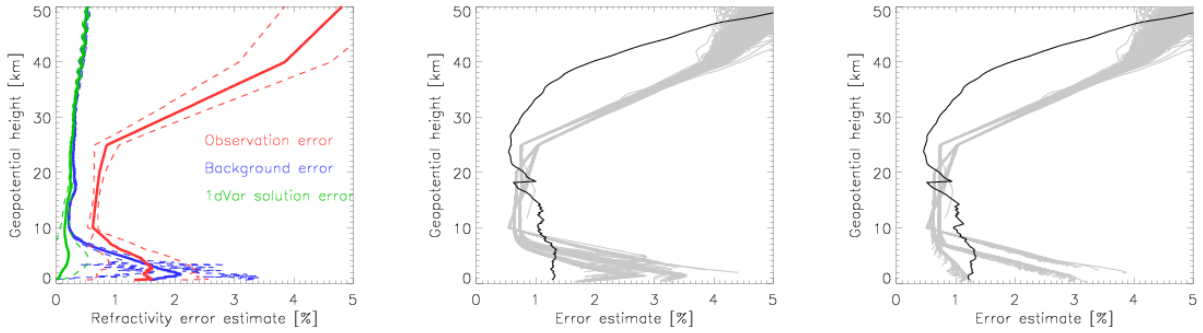

Figure 2.11: left column: Mean refractivity error estimates on observation, background and solution profiles. middle column: Error estimates on $(O-B)/B$ for each profile computed by Equation 2.6 (thin grey lines) compared with the calculated $(O-B)/B$ standard deviation (black line). right column: As in middle column but for deviation of the solution (A) from the observations $(O-A)/A$.

2.5 Results: GRAS bending angle, ECMWF background

Tests were also conducted using the `ropp_1dvar_bangle` tool to perform a 1dVar retrieval using GRAS bending angle observations. The results are similar to those previously discussed using refractivity observations. Figure 2.12 provides some summary plots of output using the default test setup with `LevMarq` minimisation.

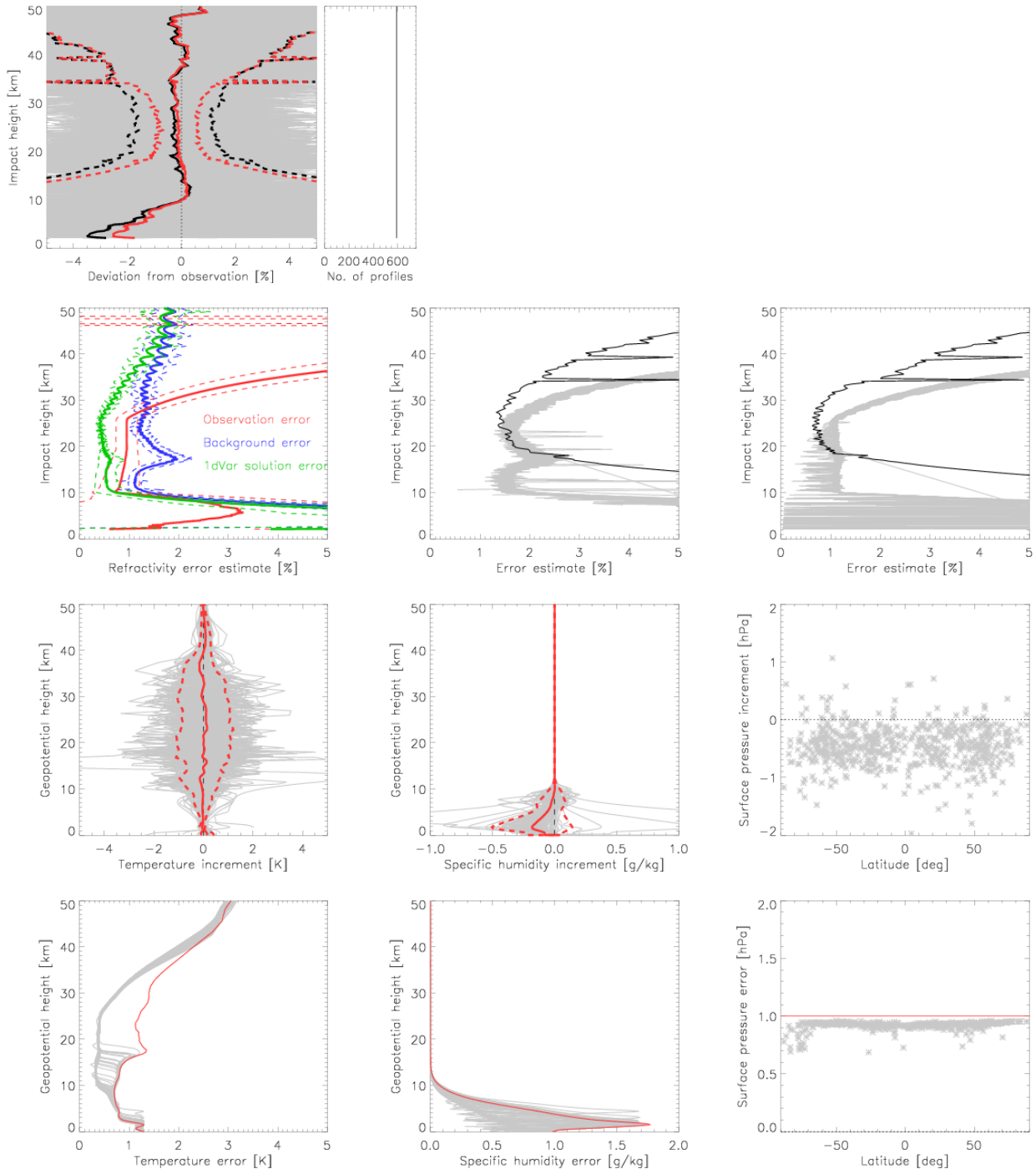

Figure 2.12: Summary of 1dVar results using GRAS bending angle observations and ECMWF background. 1dVar using (p,q) state vector variable and `LevMarq` minimiser. See Figures 2.1, 2.4 and 2.11 for plot details.

2.6 Results: GRAS refractivity, Met Office background

Observations from a day of GRAS occultations were also used in a 1dVar retrieval with Met Office forecast model background data. Pressure and specific humidity are used in the state vector and the background is on height-based model levels. Observation and background errors are a function of latitude. Figure 2.13 summarises the results. The conservative background errors leads to relatively small increments from the background in the 1dVar solution.

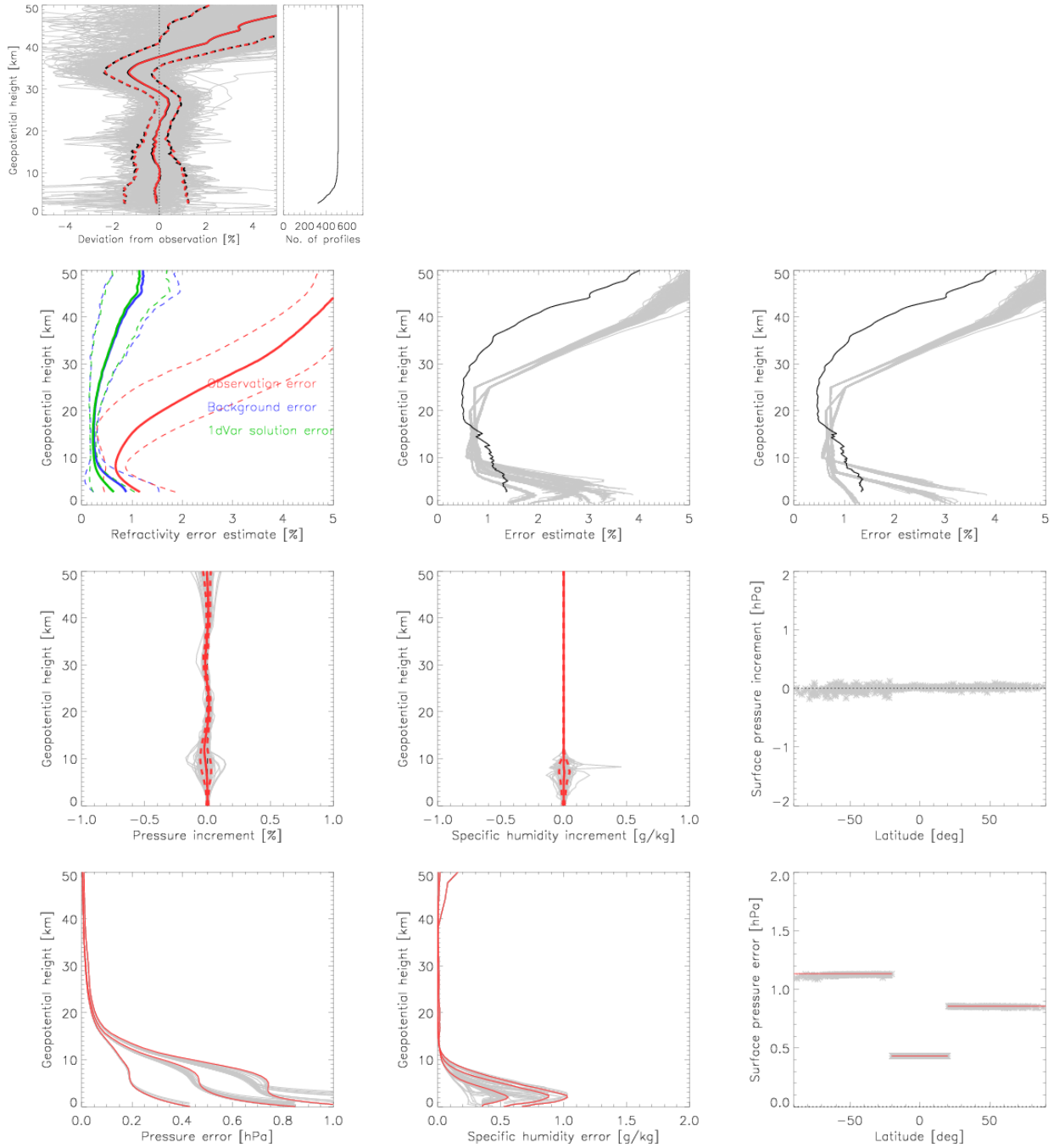

Figure 2.13: Summary of 1dVar results using GRAS refractivity observations and Met Office background. 1dVar using (p,q) state vector variable and `LevMarq` minimiser. See Figures 2.1, 2.4 and 2.11 for plot details.

2.7 Results: COSMIC refractivity, Met Office background

Figure 2.14 summarises the results of running `ropp_1dvar_refrac` using a day of refractivity observations from COSMIC and collocated Met Office background data. Observations between 0 km and 35 km are used in the retrieval. Results are generally similar to those using data from GRAS, although the inclusion refractivity data processed using wave optics in the lower troposphere leads to increased specific humidity increments.

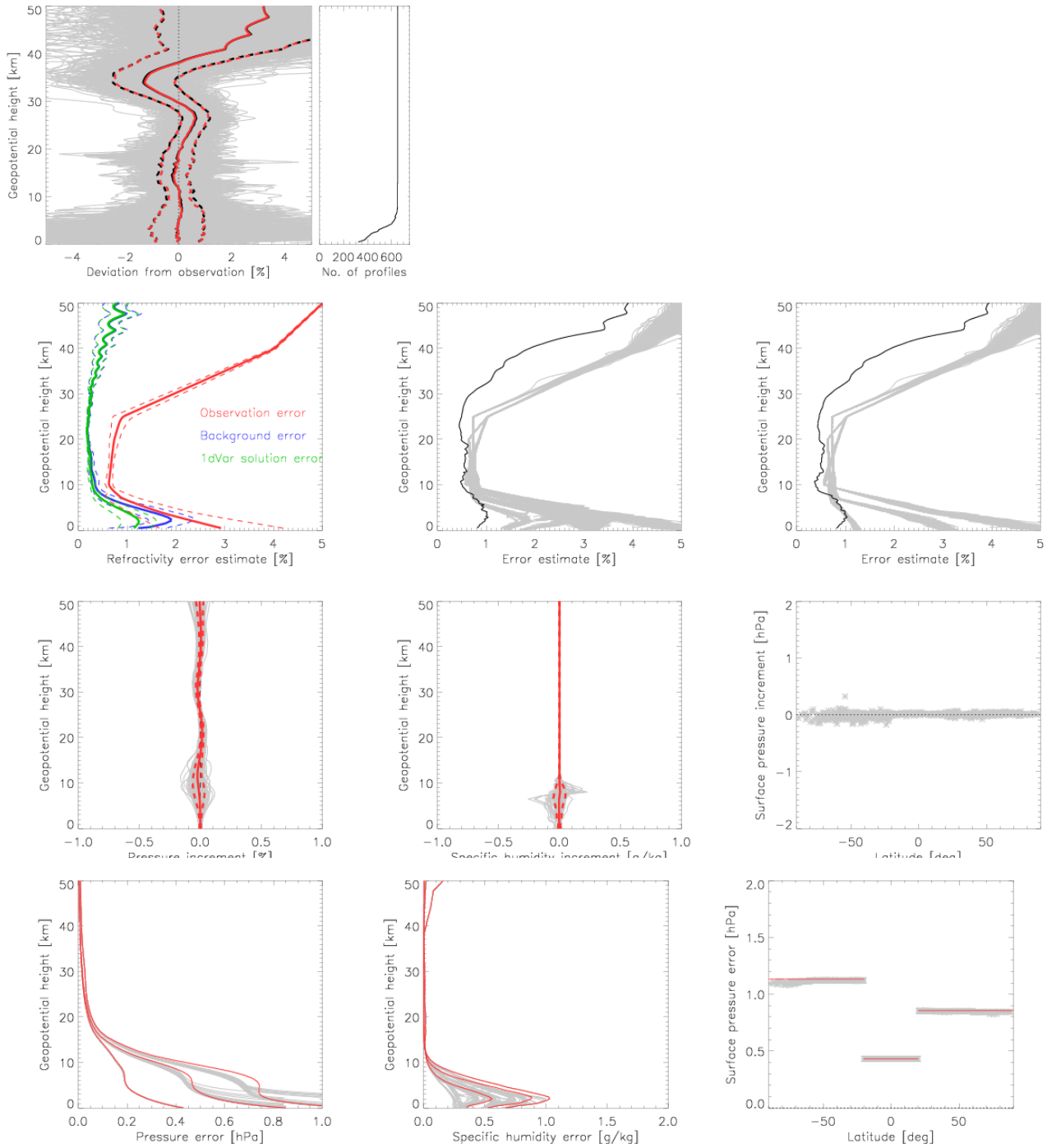

Figure 2.14: Summary of 1dVar results using COSMIC refractivity observations and Met Office background. 1dVar using (p,q) state vector variable and `LevMarq` minimiser. See Figures 2.1, 2.4 and 2.11 for plot details.

3 Summary

A series of 1dVar tests have been conducted to demonstrate the application of the ROPP 1dVar tools and algorithms to retrieve temperature, humidity and pressure information from radio occultation observations. The ROPP 1dVar processing is used to generate the GRAS SAF NRT temperature, specific humidity, pressure and surface pressure products (GRM-02, GRM-03, GRM-04, GRM-05).

One of the main outcomes of this study is the sensitivity of near-surface specific humidity generated using the `minROPP` minimiser to the preconditioning. Users should be aware that one method of preconditioning is not necessarily appropriate for all choices of the background covariance matrix. The `LevMarq` minimisation method does not require preconditioning, and is therefore considered more appropriate for most 1dVar applications. It is intended that 'K-code' functionality in the `ropp_fm` forward model module will be provided in a future update release (ROPP-5), which will improve the efficiency of the 1dVar using `LevMarq`.

A second outcome is an understanding of the negative surface pressure increments found for 1dVar retrievals using ECMWF background data. A number of tests show that these are consistent with known biases between the ECMWF background and observations. The updated COSMIC processing after 13th October 2009 has led to decreased surface pressure increments. Further changes should be expected after modifications to the treatment of aircraft temperatures in the ECMWF assimilation system. This study highlights the utility of the ROPP 1dVar tools for testing the impact of model and observation processing changes on retrieved profiles. The sensitivity of surface pressure increments to biases in the ECMWF background is much greater than found for retrieved temperature or specific humidity profiles, and these data (GRAS SAF product GRM-05) should therefore be treated with caution by users.

Bibliography

Lorenc, A., Analysis methods for numerical weather prediction, *Quart. J. Roy. Meteorol. Soc.*, *112*, 1177–1194, 1986.

GRAS SAF, Levenberg-Marquardt minimisation in ROPP, SAF/GRAS/METO/REP/GSR/006, 2008.

GRAS SAF, The Radio Occultation Processing Package (ROPP) User Guide. Part II: Forward model and 1dVar modules, SAF/GRAS/METO/UG/ROPP/003, Version 4.0, 2009a.

GRAS SAF, The Radio Occultation Processing Package (ROPP) User Guide. Part I: Input/Output module, SAF/GRAS/METO/UG/ROPP/002, Version 4.0, 2009b.

GRAS SAF, 1d-var Algorithm Document, SAF/GRAS/DMI/ALG/1DV/001, Version 2.1, 2009c.

GRAS SAF, Validation Report: GRM-02, GRM-03, GRM-04, GRM-05: NRT 1dVar profiles, SAF/GRAS/DMI/RQ/REP/002, Version 1.1, 2009d.

GRAS SAF Reports

SAF/GRAS/METO/REP/GSR/001	Mono-dimensional thinning for GPS Radio Occulation
SAF/GRAS/METO/REP/GSR/002	Geodesy calculations in ROPP
SAF/GRAS/METO/REP/GSR/003	ROPP minimiser - minROPP
SAF/GRAS/METO/REP/GSR/004	Error function calculation in ROPP
SAF/GRAS/METO/REP/GSR/005	Refractivity calculations in ROPP
SAF/GRAS/METO/REP/GSR/006	Levenberg-Marquardt minimisation in ROPP
SAF/GRAS/METO/REP/GSR/007	Abel integral calculations in ROPP
SAF/GRAS/METO/REP/GSR/008	ROPP thinner algorithm
SAF/GRAS/METO/REP/GSR/009	Refractivity coefficients used in the assimilation of GPS radio occultation measurements
SAF/GRAS/METO/REP/GSR/010	Latitudinal Binning and Area-Weighted Averaging of Irregularly Distributed Radio Occultation Data
SAF/GRAS/METO/REP/GSR/011	ROPP 1dVar validation

GRAS SAF Reports are accessible via the GRAS SAF website http://www.grassaf.org.